Supplementary Information

The Metabolome Weakens RNA Helix Stability and Increases RNA Chemical Stability

Jacob P. Sieg[¶1,2], ¶ Lauren McKinley, Melanie Huot, Neela Yennawar, and Philip C. Bevilacqua*[1,2,3]

[1]Department of Chemistry, Pennsylvania State University, University Park, PA 16802.

[2]Center for RNA Molecular Biology, Pennsylvania State University, University Park, PA 16802.

[3]Department of Biochemistry and Molecular Biology, Pennsylvania State University, University Park, PA 16802.

Keywords

Magnesium ion, Metabolites, Chelated magnesium, RNA folding, RNA function, near-cellular condition

ORCID:

Philip C. Bevilacqua: 0000-0001-8074-3434

Jacob P. Sieg: 0000-0001-5414-1667

*Corresponding author

Commented [SJP1]: Have them add their own affiliations

Commented [SJP2]: Have co authors add ORCID

Contents……

Supplementary information methods

Reagent preparation

Buffers were prepared by dissolving salts in purified (18 mΩ) water in volumetric flasks, at the purity specified in Supplementary Table 1. All reagents contained a background of 20 mM MOPS, 0.01 mM EDTA, 0.001% (w/v) SDS, pH 7 buffer unless otherwise stated. Small amounts of EDTA were present to sequester trace divalent metal ion contamination. Small amounts of SDS were present to prevent RNA from sticking to tubes/pipette tips and to protect RNA from enzymatic degradation. To ensure accurate magnesium chloride concentrations, solutions were prepared by diluting standard 1.00 M (±0.01) magnesium chloride solution from Sigma into buffer, or magnesium chloride hexahydrate was dissolved in buffer and then the concentration was determined with atomic absorption spectroscopy.

Data analysis and transparency. Data analysis was performed in R (version 4.1.0) with the *tidyverse* package for data wrangling and plotting. Unless otherwise stated, non-linear regression was performed with the *nls* function and linear regression was performed with the *lm* function in base R. The packages *MuMin*, *ggpubr*, *viridis*, *ggbeeswarm*, and *cowplot* were used to evaluate polynomial fits, display statistics, generate color-blind-friendly palettes, make beeswarm plots, and arrange figure panels, respectively. All raw data and analysis code is available with instructions for reconstitution on any console at (URL provided at submission) and archived at (URL provided upon submission).

Apparent Mg^{2+} binding constant determination with isothermal titration calorimetry

Samples were degassed using a ThermoVac (MicroCal, LLC) degasser before loading into a VP-ITC MicroCalorimeter (MicroCal, LLC) according to the manufacturer's recommendations, with pure (18 MΩ*cm) water in the reference cell. Titration was performed with a 10 µcal/sec reference power and a stirring speed of 310 rpm. Twenty-nine injections (one 2 µL injection followed by twenty eight 10 µL injections) were performed in total at an injection rate of 0.5 µL/sec with a 150 sec equilibration period following each injection. The first injection was not included in subsequent analysis. Data were analyzed using ITC parsing and non-linear regression fitting functions in MetaboMgITC (https://github.com/JPSieg/MetaboMgITC2).

Determination of Mg^{2+} speciation with HQS fluorescence

8-Hydroxy-5-quinolinesulfonic (HQS) acid hydrate (98% purity) was purchased from Sigma Aldrich and recrystallized in water 10 times to remove trace metal contamination. Purified HQS was dissolved in buffer to a stock concentration of 100 mM (determined with UV absorbance using $\varepsilon_{326\ nm}$ = 2600 $M^{-1}cm^{-1}$). HQS was then diluted to a final concentration of 50 µM with variable concentrations of Mg^{2+} and metabolites with a final sample volume of 100 µL. Control samples contained 240 mM NaCl and 140 mM KCl.

HQS emission was measured with a Biotek Cytation 3 plate reader with and excitation of 355 nm and emission of 500 nm. Plates sealed with transparent PCR film and were incubated at 37 °C for 10 min prior to reading to ensure thermal equilibration.

Fluorescence data in the absence of metabolite chelators were fit to Equation 1, in order to determine the inverse molar apparent association constant for HQS binding to Mg^{2+} (K_{HQS}).

Commented [SJP3]: Phil: "Correct?"
Jacob: Yes this is correct

Commented [SJP4]: Update version in final draft. Also need to cite packages.

Commented [SJP5]: Cite

Commented [SJP6]: Clean up V2 and cite our review.

Commented [SJP7]: Phil: "That's it, 260?"

Jacob. No. It is 2600. Cite. Check lab notebook.

Commented [SJP8]: Double check

$$\text{Emission} = (I_{max} - I_{min})\left(\frac{K_{HQS} * [Mg]}{1 + K_{HQS} * [Mg]}\right) + I_{min} \quad (1)$$

[Mg] is the free Mg^{2+} concentration in the sample, which is equal to the total concentration of magnesium chloride in the absence of chelators. I_{max} and I_{min} are the intensity of the Mg^{2+}-HQS complex and the intensity of free HQS, respectively. The fluorescence for all samples were normalized using I_{max} and I_{min} to produce a normalized fluorescence intensity I_{norm}.

$$I_{norm} = \left(\frac{\text{Emission} - I_{min}}{I_{max} - I_{min}}\right) \quad (2)$$

Free Mg^{2+} concentrations for each sample were calculated with Equation 3, using I_{norm} and K_{HQS}.

$$[Mg] = \left(\frac{I_{norm}}{K_{HQS}(1 - I_{norm})}\right) \quad (3)$$

Apparent Mg^{2+} binding constant determination with HQS

Metabolite concentrations were 240 mM for HQS experiments to determine apparent binding constants, and extra NaCl or KCl was added to maintain a constant total monovalent metal ion concentration of 240 mM Na^+ and 140 mM K^+. Metabolite solutions were treated with chelex resin to remove divalent ion contamination. The solution was passed through a 0.2 µm filter and the pH was readjusted to 7.0. The free Mg^{2+} concentration in the presence of chelators versus the total Mg^{2+} was fit to Equation 4.

$$[Mg] = [Mg]_T - \frac{\left([Mg]_T + [L]_T + \frac{1}{K'}\right) \pm \sqrt{\left([Mg]_T + [L]_T + \frac{1}{K'}\right)^2 - 4[Mg]_T[L]_T}}{2} \quad (4)$$

Where $[Mg]_T$ is the total Mg^{2+} concentration, $[L]_T$ is the metabolite concentration, and K′ is the apparent ligand binding constant for Mg^{2+}, represented by Equation 5.

$$K' = \frac{[MgL]}{[Mg][L]} \quad (5)$$

Determination of total Mg^{2+} required to have 2 mM free Mg^{2+} in artificial cytoplasm

The total Mg^{2+} concentration required to have 2 mM free in artificial cytoplasm was approximated using the free Mg^{2+} concentrations calculated using HQS data. The free Mg^{2+} concentration, which was measured as a function of the total Mg^{2+}, were fit to 1st, 2nd, 3rd, 4th , 5th , 6th, 7th, 8th, 9th and 10th order polynomials in the form:

$$[Mg] = \sum_{i=1}^{N} A_i [Mg]_T^{\,i} + C \quad (6)$$

Where *N* is the order of the polynomial and *A/C* are constants determined by linear regression. Fit polynomials were evaluated by calculating the Akaike information criterion (AIC), in order to determine which polynomial best described the data using the minimum number of terms. The polynomial with the lowest AIC was then solved numerically to calculate the total Mg^{2+} required

to generate 2 mM free Mg^{2+} in the presence of metabolites, with a tolerance of 0.01 mM. The fluorescence of control samples containing 10 mM EDTA was compared to the no added magnesium chloride condition to determine divalent metal ion contamination levels in artificial cytoplasm, which was a negligible amount of signal, less than the signal produced by 0.3 mM free Mg^{2+}.

Artificial cytoplasm preparation

Artificial cytoplasm was prepared to maintain a constant monovalent ion concentration of 240 mM Na^+ and 140 mM K^+ and a pH of 7. First, metabolite salts or solutions were dissolved or diluted into water in volumetric flasks. Second, the pH of each solution was adjusted to 7.0 using 10 M NaOH. The amount of Na^+ or K^+ added with each component was recorded. Third, 5 M NaCl and 2 M KCl were added for a final Na^+ and K^+ concentration of 480 mM and 280 mM, respectively. Then, the volumetric flask was filled with water to 10 mL. Lastly, a test quantity of the 2x solution was diluted to a 1x concentration and the pH was tested with a VWR Symphony pH probe. The 2x concentrated artificial cytoplasm was aliquoted, stored at -20 °C. A detailed recipe for the Eco80 artificial cytoplasm is available in SI Table 1. Periodically, the artificial cytoplasm was spot checked for NTP degradation using thin-layer chromatography on PEI plates developed with a 0.3 M potassium phosphate mobile phase.

Single-binding-site statistical model for Mg^{2+} speciation in artificial cytoplasm

We used a statistical model, that considers experimental errors in metabolite/Mg^{2+} concentrations and uncertainties in apparent binding constant determination, to calculate the expected free Mg^{2+} concentration in artificial cytoplasm, assuming single-site binding (meaning one metabolite molecule binds one Mg^{2+} and vice-versa). Single site binding of a metabolite to Mg^{2+} is described by the apparent dissociation constant (K_D').

$$K_D' = \frac{[L][Mg]}{[MgL]} \quad (7)$$

Rearranging to determine the concentration of the metabolite-ligand complex [MgL] as a function of the concentration of free Mg^{2+}, and the total ligand concentration ($[L]_T$), we get equation 8.

$$[MgL] = \frac{[L]_T[Mg]}{K_D' + [Mg]} \quad (8)$$

In a mixture of metabolites, the total Mg^{2+} will be the free Mg^{2+}, plus the Mg^{2+} bound by different metabolites.

$$[Mg]_T = [Mg] + \sum_{i=1}^{N} [MgL_i] \quad (9)$$

Where N is the total number of metabolites in the solution. Equation 8 was plugged into Equation 9 to obtain the total Mg^{2+} as a function of the free Mg^{2+}, the apparent dissociation constant, and the total metabolite concentration in global metabolite mixtures.

Commented [SJP11]: Phil: "Do you mean Cl-?"

Jacob: No. This is an interesting point that I don't have my mind wrapped around. But there is something profound here. Here are two things I am thinking about.

(1) Metabolites were ordered as either Na or K salts. It is not possible to get to 240 mM Na 140 mM K pH 7.0 using only Na salts for E. coli metabolite concentrations because there has to be electroneutrality. If you tried using only sodium, you would go beyond 240 mM Na.

(2) Eukaryotes, have much less NTPs, which come as a charge of -2 to -3. I have not tried, but according to math, it is possible to make something like a Mammalian imbk 80 artificial cytoplasm with solely 240 mM Na at pH 7. Likewise, Eukaryotes are generally thought to have much less K in the cell, like 10 mM.

(3) Essentially what we are doing here is replacing Cl anions with metabolite anions. And this is destabilizing to RNA secondary structure.

Commented [SJP12]: Check vendor

$$[Mg]_T = [Mg] + \sum_{i=1}^{N} \frac{[L_i]_T[Mg]}{K'_{D_i} + [Mg]} \quad (10)$$

The total Mg^{2+} and the total metabolite concentrations are set in the experiment, and the apparent dissociation constants were determined with ITC or HQS fluorescence. Thus, the expected free Mg^{2+} was determined to a precision of 0.01 mM by solving equation 10 numerically (possible because equation 10 has one real solution between 0 free Mg^{2+} and the total Mg^{2+} concentration in the solution).

Expected experimental error was calculated by propagating uncertainties in mass and volume during sample preparation. Briefly, equation 11 and 12 was used for propagation of uncertainty for addition and multiplication/division respectively.

$$\text{For } A = B + C \text{ or } B - C \left\{ dA = \sqrt{dB^2 + dC^2} \right\} \quad (11)$$

$$\text{For } A = B * C \text{ or } A = \frac{B}{C} \left\{ dA = A\sqrt{\left(\frac{dB}{B}\right)^2 + \left(\frac{dC}{C}\right)^2} \right\} \quad (12)$$

The percent impurities (supplied by the chemical vendor) were used as the uncertainty for mass measurements because the uncertainty from the impurity was greater than the precision of our analytical balance (0.1 mg). Volume uncertainties were provided by the manufactures of the pipettes and volumetric flasks. For metabolites, uncertainty in concentration was on average 9.1 % of the final concentration in artificial cytoplasm. For total Mg^{2+}, the uncertainty was on average 5%. Thus we used 10% and 5% uncertainty for metabolite and total Mg^{2+} concentrations.

Commented [SJP13]: Need to calculate.

For the statistical model, random error was seeded into equation 10 using the *rnorm* function in base R, which creates random error based on a gaussian distribution with a standard deviation (σ_x) described by equation 13.

$$\sigma_x = \frac{x * \%\text{uncertainty}}{100} \quad (13)$$

The standard deviation provided by the fit was used for apparent dissociation constants. Thus, Equation 14 can be used to generate a virtual artificial cytoplasm with realistic errors in reagent concentrations.

$$[Mg]_T + \text{rnorm}(\sigma_{[Mg]_T}) = [Mg] + \sum_{i=1}^{N} \frac{\left([L_i]_T + \text{rnorm}(\sigma_{[L_i]_T})\right)[Mg]}{K'_{D_i} + \text{rnorm}\left(\sigma_{K'_{D_i}}\right) + [Mg]} \quad (14)$$

One thousand virtual artificial cytoplasm were created with Equation 14 to fully explore possible variance and the results were compared with experimental measurements of free Mg^{2+} determined with HQS.

Fluorescence binding isotherms

5´-FAM and 3´-BHQ1 labeled RNA were ordered from Integrated DNA Technology (IDT) and HPLC purified by ITD or in house. For in house HPLC, RNA peaks were manually collected on a Water's AQUINITY Arc UPLC system equipped with a Waters Xbridge C18 2.3 μm 4.6x150 mm column. 5 nmole of RNA were injected to a 60 °C preheated column and separated for 5 min with 100% 0.1 M aqueous Triethylamine acetate (TEAA), followed by a 25 min transition to 100% 0.1 M TEAA 20% acetonitrile, followed by 5 minutes of 100% 0.1 M TEAA 20% acetonitrile, and then a 5 min transition back to 100% aqueous 0.1 M TEAA, at a flow rate of 1 mL/min. Samples were dried under vacuum and resuspended in buffer. Then, samples were dialyzed twice against 1 L of buffer in an 8 well Life Technologies Microdialysis System equipped with a 1 kDa dialysis membrane (SpectraPore) for 24 hours per liter of buffer. Dialyzed RNA concentrations were determined using the absorbance at 260 nm and extinction coefficients provided by IDT. Final samples were prepared in triplicate, where FAM-RNA were diluted to 200 nM and BHQ1-RNA were diluted to 0, 1, 10, 50, 100, 150, 200, 400, 800, and 1000 nM. The 2xconcentrated salts or artificial cytoplasm were diluted into the same samples to achieve a final 1x concentration with 0.5 mM free ROX as a passive reference dye. Samples were heated to 90 °C for 1.5 min, cooled at room temperature for 20 min, transferred into a 96 well qPCR plate, sealed with transparent qPCR film, and centrifuged for 2 min to remove air bubbles. Fluorescence emission of the entire plate as a function of temperature was measured using an Applied Biosystems Step 1 Plus qPCR instrument. Samples were heated from 20 to 80 °C at a ramp rate of 0.5 °C per minute, recording fluorescence at 0.5 °C increments. ROX-normalized FAM emission was exported from the Applied Biosystems software to a flat text file.

Fluorescence binding isotherm data analysis

Fluorescence binding isotherms were fit using the *meltR.F* program in the MeltR package VX.X. MeltR performs the following data preprocessing steps before fitting:

1.) The fluorophore labeled strand concentration is optimized using the concentration optimization algorithm, described in more below.

2.) Isotherms are fit to Equation 15 to determine K_D and error in the K_D at each temperature using "nls" in base R.

$$E = E_{max} + (E_{min} - E_{max}) \frac{(K_D + [F]_T + [Q]_T) - \sqrt{(K_D + [F]_T + [Q]_T)^2 - 4[F]_T[Q]_T}}{2[F]_T} \quad (15)$$

Where E is the observed fluorescence emission, E_{max} is the fluorescence emission of the unbound fluorophore labeled RNA strand, F_{min} is the fluorescence emission of the fluorophore labeled RNA strand bond to the quencher labeled RNA strand, $[F]_T$ is the total fluorophore labeled RNA strand concentration, $[Q]_T$ is the total quencher RNA strand concentration, and K_D is the dissociation constant given by Equation 16.

$$K_D = \frac{[F][Q]}{[Q]} \quad (16)$$

Where [F] is the concentration of free fluorophore labeled RNA, [Q] is the concentration for free quencher labeled RNA, and [FQ] is the concentration of the helical complex. Initial values for E_{max} and E_{min} are estimated by taking the mean of the 20% highest readings in each isotherm and the 20% lowest readings respectively. Initial values for the K_D are provided by the user, by default 0.1 nM.

3.) K_Ds are filtered by magnitude and error, according to user specifications, to determine which isotherms are most reliable. First, K_Ds outside of a user specified range (10 to 1000 nM by default) are thrown out. Second, K_Ds are ranked by the error in the K_D. K_Ds that are below a user specified error quantile are thrown out. The default K_D error quantile file is 0.25, meaning the algorithm will keep the to 25% most accurate K_Ds, after filtering by magnitude.

4.) The most reliable K_Ds and temperatures are passed to Method 1 to make Van't Hoff plots and to calculate helix formation energies.

5.) Fluorescence data from the most reliable K_Ds and temperatures are passed to Method 2 for global fitting and to calculate helix formation energies.

Method 1 fits a Van't Hoff plot to Equation 17 to determine the enthalpy and entropy of folding.

$$\ln(K_D) = \frac{\Delta S'}{R} - \frac{\Delta H'}{RT} \tag{17}$$

Where $\Delta S'$ is the entropy of helix dissociation, $\Delta H'$ is the enthalpy of helix dissociation, R is the gas constant, T is the temperature in Kelvin.

Method 2 Globally fits raw fluorescence data to equation 18, produced by plugging equation 17 into equation 15 to determine the entropy and enthalpy of folding.

$$E = {E_{max}}^{i} + \left({E_{min}}^{i} - {E_{max}}^{i}\right) \cdot \frac{\left(e^{\left(\frac{\Delta S'}{R} - \frac{\Delta H'}{RT}\right)} + [F]_T + [Q]_T\right) - \sqrt{\left(e^{\left(\frac{\Delta S'}{R} - \frac{\Delta H'}{RT}\right)} + [F]_T + [Q]_T\right)^2 - 4[F]_T[Q]_T}}{2[F]_T} \tag{18}$$

Where *i* is the reading the data was collected, meaning that the Emax and Emin can float between readings but the $\Delta S'$ and $\Delta H'$ are required to be the same.

Helix folding energies are traditionally reported in terms of the association constant.

$$K = \frac{1}{K_D} = \frac{[FQ]}{[F][Q]} \tag{19}$$

Thus, the entropy and enthalpy of helix association, ΔS and ΔH, are obtained by multiplying the $\Delta S'$ and $\Delta H'$ by negative 1.

MeltR reports standard error (SE) estimates provided by the non-linear model generated with the *nls* function in base R. The Gibbs free energy of helix association at 37 °C ($\Delta G^{37°C}$) is calculated with Equation 20.

$$\Delta G^{37°C} = \Delta H - 310.15\Delta S \tag{20}$$

Error in the entropy and enthalpy of helix association are calculated with Equation 21.

$$SE_{\Delta G^{37°C}} = \sqrt{SE_{\Delta H}{}^2 + (310.15SE_{\Delta S})^2 - 620.3\frac{\sigma_{\Delta H,\Delta S}}{\Delta H, \Delta S}} \tag{21}$$

Where $\sigma_{\Delta H,\Delta S}$ is the covariation between the ΔS and ΔH given by *nls* in base R. Additional error analysis is described below.

MeltR concentration optimization algorithm

We found that helix energies from fitting fluorescence binding isotherms are highly dependent on the errors in the determination of RNA concentrations in stock solutions, which is propagated systematically during sample preparation. For example, if the FAM-RNA stock actually more 20% concentrated than the estimate calculated using UV absorbance and extinction coefficients would suggest, the FAM-RNA concentration in the final samples will be consistently 20% higher because the same amount of master mix is added to each sample (SI Figure 3), which can bias the resulting helix folding energies. To understand why, we modeled data assuming a folding enthalpy (ΔH), entropy (ΔS), and Gibb's free energy at 37 °C ($\Delta G^{37°C}$) of -56.2 kcal/mol, -136.4 cal/mol/K, and -13.9 kcal/mol respectively, 5% random fluorescence error, and perfectly accurate determination of RNA concentrations in concentrated stocks (a 200 nM FAM-RNA concentration, and 0, 1, 10, 50, 100, 150, 200, 250, 400, 600, 800, and 1000 nM RNA-BHQ1 concentrations). We then used MeltR to fit the modeled data, resulting in a very accurate determination of ΔH = -56.0 kcal/mol, ΔS = -135.7 cal/mol/K, and $\Delta G^{37°C}$ = -13.9 kcal/mol. We next considered how assuming incorrect RNA stock concentrations, thus incorporating a systematic error, could effect the accuracy of the fits. Systematic error (-50% to +50%) was seeded into virtual stock concentrations and the data were refit (SI figure XA). We found that fit accuracy what highly dependent on error in stock concentrations. For example, if the FAM-RNA concentration in the stock is 25% lower than the estimate, and the RNA-BHQ1 concentration is 25% higher than the estimate, the $\Delta G^{37°C}$ that MeltR calculated is about 4 kcal/mol off. Likewise, if the FAM-RNA concentration in the stock is 25% higher than the estimate, and the RNA-BHQ1 concentration is 25% lower than the estimate, the $\Delta G^{37°C}$ that MeltR calculated is about 2.5 kcal/mol off. However, if the FAM-RNA error and the RNA-BHQ1 error compensate for each other, e.g. %RNA-BHQ1 error = %FAM-RNA error, the the $\Delta G^{37°C}$ that MeltR calculates is less than 0.2 kcal/mol off, even with 50% inaccuracy in RNA stock concentrations (a two fold increase or decrease).

We next considered a more realistic scenario, where the experiment assumes perfectly accurate determination of RNA concentrations but there is actually +20% FAM-RNA concentration error. Data was modeled using the same folding energies and RNA-BHQ1 concentrations, but with a 240 nM FAM-RNA concentration (+20% error). We then used MeltR to fit the modeled data, assuming a 200 nM FAM-RNA concentration, resulting in inaccurate determination of ΔH = -35.8 kcal/mol, ΔS = -75.5 cal/mol/K, and $\Delta G^{37°C}$ = -12.3 kcal/mol, a .$\Delta G^{37°C}$ error of 1.6 kcal/mol. Once again, we seeded systematic error (-50% to +50%) into virtual stock concentrations and the data were refit (SI figure 4B). Similar to SI figure 4A, we found that fit accuracy what highly dependent on errors in stock concentrations. However, the fits were most accurate according to Equation 1 instead of where %RNA-BHQ1 error = %FAM-RNA error:

$$\%BHQ1_{error} = \frac{1}{X}\%FAM_{error} + \frac{100 - 100X}{X}$$

Where X is the actual FAM-RNA concentration divided by the estimated FAM-RNA concentration (240 nM/200 nmol = 1.2 in this example). Thus, MeltR does not need perfectly accurate concentrations, just an optimization algorithm that finds the FAM-RNA concentration correction factor X. To find X, MeltR selects an isotherm (usually the lowest temperature), where the K_D is more than 10 times less than the FAM-RNA labeled concentration (SI figure 4C). At this K_D range, the shape of the binding curve is independent of K_D, and MeltR uses the isotherm as a Job plot to determine X. MeltR then uses X to correct the FAM-RNA concentration. We next tested the MeltR optimization algorithm. The modeled data, with an uncorrected +20% FAM-RNA concentration error, was fit using MeltR with the concentration optimization algorithm on, resulting in an accurate determination of ΔH = -51.9 kcal/mol, ΔS = -123.5 cal/mol/K, and $\Delta G^{37^\circ C}$ = -13.6 kcal/mol, a $\Delta G^{37^\circ C}$ error of 0.3 kcal/mol. We then seeded additional error into the data set (-50% to +50%), refit the data using the MeltR concentration optimization algorithm, and found that MeltR calculates accurate folding energies (within 0.2 kcal/mol in terms of the ΔG) even with large inaccuracies in reagent concentration estimates (SI Figure 4D).

MeltR then filters out isotherms that produce inaccurate K_Ds, according to user specifications (see above). Both the MeltR K_D range, and K_D error threshold can be adjusted by the user in real time to refine fits by manually inspecting Van't Hoff plots to identify the most accurate temperature range to fit. For example, the MeltR fit of the modeled data can be improved to ΔH = -56.4 kcal/mol, ΔS = -136.9 cal/mol/K, and ΔG = -13.9 kcal/mol using the concentration optimization algorithm and by selecting the most accurate temperature range by inspecting the Van't Hoff plot.

Helix folding energy error analysis

Standard errors estimated from the fit for method 1 were 1.7%, 2%, and 0.3 % on average for the ΔH, ΔS, and $\Delta G^{37^\circ C}$. Standard errors estimated from the fit for method 2 were larger, at 21.7%, 26.5%, and 3.4 % on average for the ΔH, ΔS, and $\Delta G^{37^\circ C}$. However, the difference in helix folding energies between the two methods between the two methods was much smaller, at 1.2%, 1.4%, and 0.2% on average for the ΔH, ΔS, and $\Delta G^{37^\circ C}$. Given that the two methods provide similar helix folding energies, but different standard errors, the discrepancy in standard error likely reflects differences in the number of parameters that must be estimated by the fit (two for method 1, ΔH and ΔS, and 2+2*number of raw isotherms for method 1, ΔH, ΔS, and a F_{max}/F_{min} for each raw isotherm), more than it reflects systematic and random errors in helix folding energy estimation. Turner and colleagues estimated an uncertainty of 12%, 13.5%, and 4% for the ΔH, ΔS, and $\Delta G^{37^\circ C}$, respectively, conservatively reflect systematic and random errors in error determination for absorbance melting curves by comparing helix energies collected on the same sequences by different labs. Given that the discrepancy between method 1 and method 2 were smaller than the Turner uncertainty for all fluorescence binding isotherms in this study, and that we are determining differences between conditions on the same sequences collected in the same lab, the 4% value in terms of the is too conservative. We determined that there was on average 0.2 kcal/mol, or 1.5%, error for MeltR fitting modeled fluorescence data using the concentration optimization algorithm (SI Figure 4). Thus, we reported the $\Delta G^{37^\circ C}$ of helix formation from method 1 with an uncertainty of 1.5% in Table 3 and the 1.5% uncertainty was propagated to the association constant in Figure 2D.

RNA transcription and purification

$tRNA^{Phe}$ was transcribed from7 µM hemiduplex DNA and Guanine aptamer/CPEB3 ribozymes were transcribed from duplexes prepared with polymerase chain reaction (PCR) reactions (Supplementary table X). PCR was performed with Taq polymerase (New England Biolabs) and cleaned up with a RNA clean and concentrate kit (Zymogen), according the manufacturers instructions. For cleaning up large scale PCR to make template for SAXS experiments, polymerase was removed with an equal volume 25:24:1 phenol:chloroform:isoamyl alcohol extraction, and two subsequent equal volume 24:1 chloroform:isoamyl alcohol extractions. The dNTPs were removed using an ethanol precipitation with ~ 2 M ammonium acetate and >75% ethanol. Transcription reactions were performed with in-house prepared T7 polymerase at 37 °C for 3 hr, with 4 mM ATP, 4 mM CTP, 4 mM UTP, 8 mM GTP, 25 mM $MgCl_2$, 0.1 mM spermidine, 2 mM dithioritol, 20 mM Tris pH 8.0. NTP stocks were preadjusted to pH 8.0 with Tris base. Transcriptions were stopped with the addition of EDTA to a final concentration of 50 mM and cleaned up using phenol:chloroform:isoamyl alcohol extractions (as described for the

PCR clean up) followed by ethanol precipitations containing ~2 M ammonium acetate and >75 % ethanol. RNA were resuspended in 50% formamide with 25 mM EDTA (pH 8.0), heated to 90 °C, and loaded hot onto a denaturing (8.3 M urea) 10% (g/mL) acrylamide gel containing 1xTBE. Full length RNA bands were identified with UV-shadowing, excised, and electroeluted (Elutrap, Whatman) according to the manufactures recommendation. Electroluted RNA were concentrated with an ethanol precipitation containing ~0.8 M LiCl and >75 % ethanol, resuspended in buffer, and stored at -20 °C.

For 5´-end labeling, the 5´-triphosphate on the transcription product was removed from about 10 pmol of RNA using shrimp alkaline phosphatase SAP (New England Biolabs). SAP was heat inactivated by incubating at 72 °C for 5 min. RNA from the SAP reactions were 5´-^{32}P labeled with 0.5 to 3.5 µM γ-^{32}P-ATP using T4 Polynucleotide kinase (New England Biolabs) according to the manufactures recommendation. Kinase reactions were stopped with an equal volume of 90% formamide with 50 mM EDTA pH 8.0 loading dye containing trace xylene cyanol and bromophenol blue. Kinased products were excised from a denaturing (8.3 M urea) 10% (g/mL) acrylamide gel containing 1xTBE, crush and soaked overnight in TEN_{250} at 4 °C, ethanol precipitated, and resuspended in 100 µL buffer. For internal (body) labeling, RNA were transcribed with an additional 2 µL of source and purified as described for the kinase reaction.

In-line probing chemical stability assays. For in-line probing (ILP) degradation assays, 5 to 10 kcpm/µL 5´-^{32}P labeled RNA was incubated in triplicate at 37 °C on a PCR block. Time points were taken at 0, 2 and 4 days by quenching 10 µL of reaction in 10 µL of 95% formamide containing 50 mM EDTA pH 8.0 buffer with trace xylene cyanol and bromophenol blue. Then, 3 µL of sample were fractionated on a denaturing (8.3 M urea) 10% (g/mL) acrylamide gel containing 1xTBE. The gel was dried, exposed on a phosphoimager cassette, and scanned with a Typhoon Phosphoimager. Gels images were quantified with SAFA three times to capture variance between qualifications. Time points were corrected for background degradation at each band by subtracting out the band intensity at time 0. The change in counts with time was determined by a simple linear fit at each band (y = mx + b).

Small angle x-ray scattering (SAXS)

Transcribed and purified RNA was dialyzed twice against 1 L of buffer containing 2 mM $MgCl_2$ in an 8 well Life Technologies Microdialysis System equipped with a 1 kDa dialysis membrane (SpectraPore) for 24 hours per liter of buffer. RNA were renatured at 80 °C for 1.5 min and cooled to room temperature for 20 min. About 700 µg of RNA were ran on a [insert instrument name] equipped with a [insert column name] at 4 °C to purify RNA in the monomer conformation, with the dialysis buffer as the mobile phase. The correct molecular weight of monomers was confirmed using an in-line [insert spectrometer name] multiangle light scattering (MALS) instrument. Monomers were then diluted, to 100 µg/mL, in artificial cytoplasm with Mg^{2+}. RNA were incubated at 37 °C for 1 hour before SAXS data acquisition. [Neela can describe data acquisition and preprocessing, I am still working more collection and analysis].

Self-cleaving assay. Internal (body) ^{32}P labeled pre-CPEB3 ribozyme was diluted into artificial cytoplasm to a final concentration of 250 cpm/µL. RNA were renatured at 95 °C for three minutes then cooled in a 37 °C heat block for 10 min. Reactions were initiated by adding a 1/10 volume of a 10x$MgCl_2$, stock and time points were taken by quenching 4 µL of reaction in 4 µL of 50 mM EDTA pH 8.0 90% formamide with trace xylene cyanol and bromophenol blue. Then,

Commented [SJP14]: Lauren, can you fill out details?

Commented [SJP15]: Define

Commented [SJP16]: Ask Lauren for details.

Commented [SJP17]: citation

Commented [SJP18]: Phil: Why, It's math on the same data?

Jacob: SAFA performs a number of steps that are idiosyncratic, in particular the alignment step. Since my cleaved was so weak (pH 7.0 and low free Mg) I quantified the gel more than once to see how reproducible it was. I did see variance between quantifications so I quantified everything three times.

I do not think it is necessary for kinetics because the bands are strong and there are only two of them

Commented [SJP19]: Neela, can you describe data collection and data preprocessing (to the .out file)?

4 µL of sample were fractionated on a denaturing (8.3 M urea) 10% (g/mL) acrylamide gel containing 1xTBE. Gels were dried and imaged with a PhosphorImager (Typhoon 650; GE Healthcare) and quantified once with ImageQuant (GE Life Sciences). The fraction cleaved (*f*) was calculated from Equation 14, normalizing raw band intensities (*I*) for the number of As in the cleaved CPEB3 and pre-CPEB3 bands.

$$f = \frac{\frac{I_{CPEB3}}{13}}{\frac{I_{pre-CPEB3}}{21} + \frac{I_{CPEB3}}{13}} \quad (14)$$

Rates of self-cleavage were analyzed by fitting fraction cleaved to a single exponential curve (Equation 15).

$$f = A + Be^{-kt} \quad (15)$$

Where A is the Fraction of ribozyme cleaved at completion, -B is the amplitude of the observable phase, and *k* is the observed first-order rate constant for ribozymes cleaving in non-burst phase, and *t* is the time in minutes.

Commented [SJP20]: Phil: I believe A + B is the burst phase. Should there be one?

Jacob: I don't think a HDV burst phase has been observed but you would know better than me. But, there could be, because there is some magnesium in Eco80 and WMCM before the 10xMg is added because the purest dihydroxyacetone phosphate I could find from a reliable vendor was a hemi-magnesium salt. This should only be a small amount because the metabolites should sequester it. However, I looked for the burst phase. The analysis of the kinetics is preliminary but A + B is about 0 so I do not think there is a burst phase.

Supplementary information figures

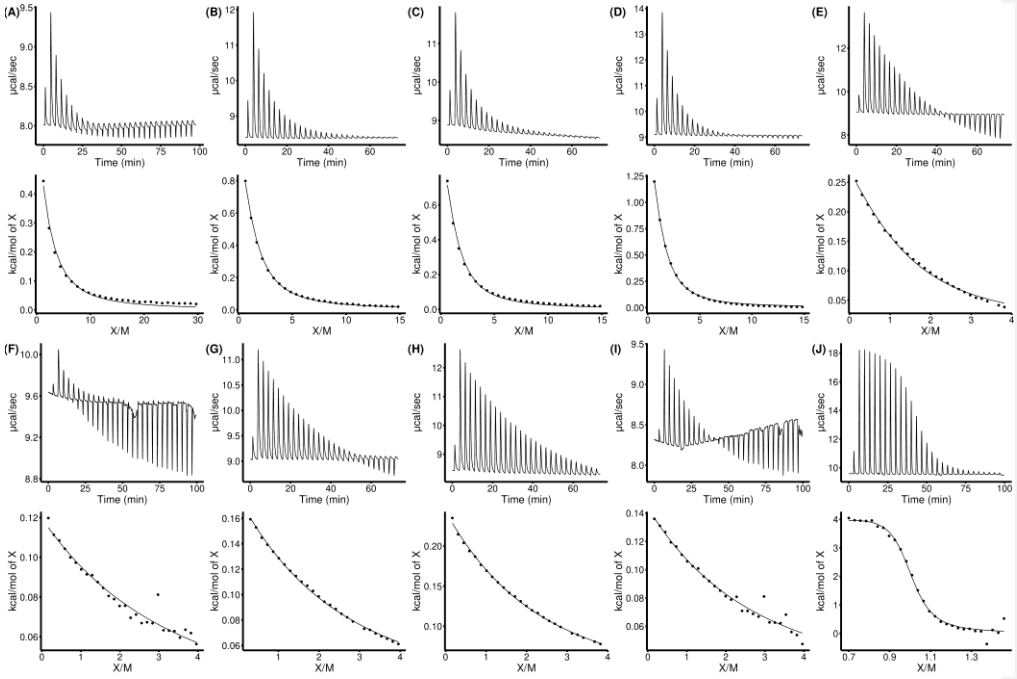

SI Figure 1 Isothermal titration calorimetry (ITC) analysis of Mg^{2+} binding to metabolites in 240 mM NaCl 140 mM KCl 10 mM HEPES pH 7.0 at 37 °C. $MgCl_2$ was titrated into metabolites and the power was monitored over time (Top panel). Heat of the injection was calculated by integrating the raw power curve, and the background heat of $MgCl_2$ dilution, collected on buffer containing no metabolite, was subtracted to produce the isotherms in the bottom panels. Lines in bottom panels represent fits to the Weismann isotherm equation to determine apparent association constants. **(A)** Adenosine triphosphate (ATP). **(B)** Uridine triphosphosphate (UTP). **(C)** Guanosine triphsophate (GTP). **(D)** deoxythymidine triphosphate (dTTP). **(E)** Fructose 1,6-bisphosphate. **(F)** Uridine diphosphate (UDP)-N-acytylglucosamine. **(G)** Glucose 6-phosphate. **(G)** 6-phosphogluconic acid. **(H)** Phosphoenol pyruvate. **(G)** Ethylene diamine-tetracetic acid (EDTA). Thermodynamic values are found in SI table 2.

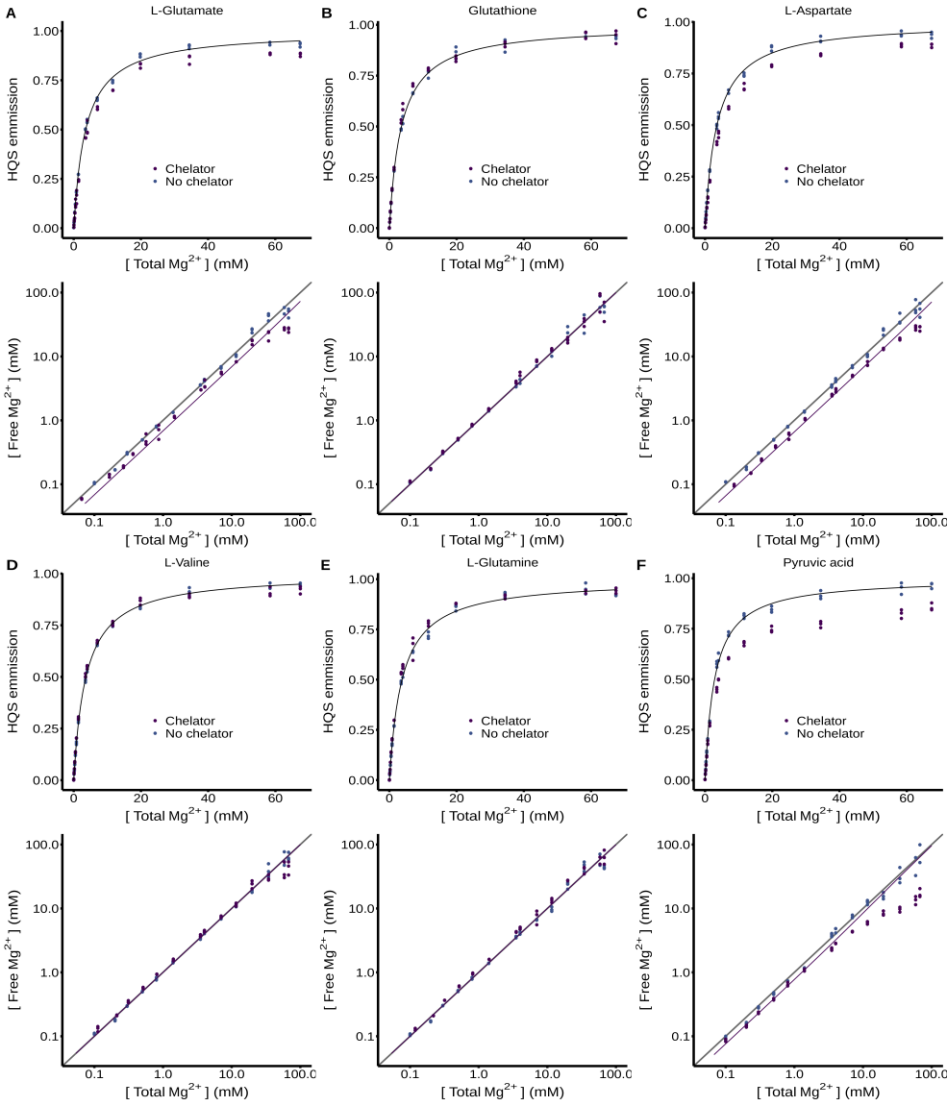

SI Figure 2 HQS analysis of Mg^{2+} binding to metabolites in 240 mM NaCl 140 mM KCl 20 mM MOPS 0.01 mM EDTA 0.001% SDS pH 7.0. (A-F Top panels) Dependence of HQS emission on the total concentration of MgCl2 in the presence and absence of a metabolite chelators. Black lines represent a fit to SI equation 1 to determine the Fmax, Fmin, and KHQS. (A-F Bottom panels) Dependence of the free Mg^{2+} concentration on the total concentration of MgCl2 in the presence and absence of a metabolite chelators. Grey lines represent where the free Mg^{2+} concentration equals the total concentration of MgCl2, Purple lines represent a fit to SI equation 4 to determine the association constant between HQS and a chelator. (A) 240 mM L-glutamate. (B) 194 Glutathione. (C) 240 mM L-aspartate. (D) 240 mM L-valine. (E) 240 mM L-glutamine. (F) 5 mM pyruvic acid.

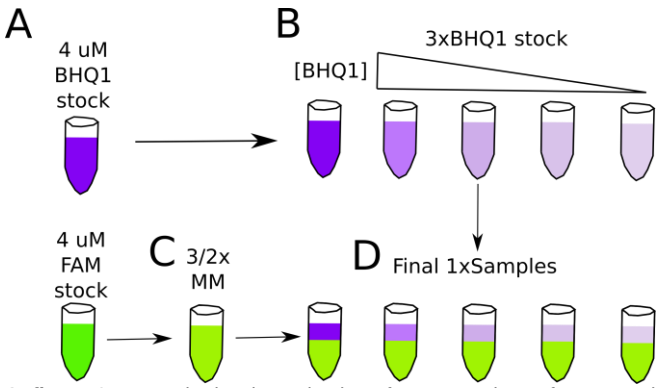

SI figure 3 Errors in the determination of concentrations of RNA stocks are systematically propagated during sample prep for fluorescence isotherm experiments. (A) FAM-RNA and RNA-BHQ1 stock concentrations are determined at a low μM concentrations with UV-absorbance. In this work, FAM and BHQ1 stocks were prepared at the same concentration, 4 μM. (B) RNA-BHQ1 stocks are diluted to a 3x concentration from one stock. (C) FAM-RNA stocks were diluted to a 3/2xconcentration into artificial cytoplasm to make a master mix (MM). (D) One volume of 3xRNA-BHQ1 stock is mixed with two volumes of 3/2xMM to prepare the final solution. Solutions appear layered in D to emphasize dilution but they are mixed to form a homogeneous solution.

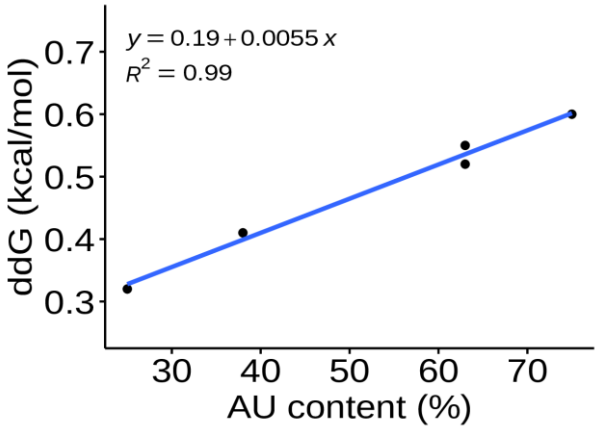

SI figure 4 Helix destabilization versus AU content.

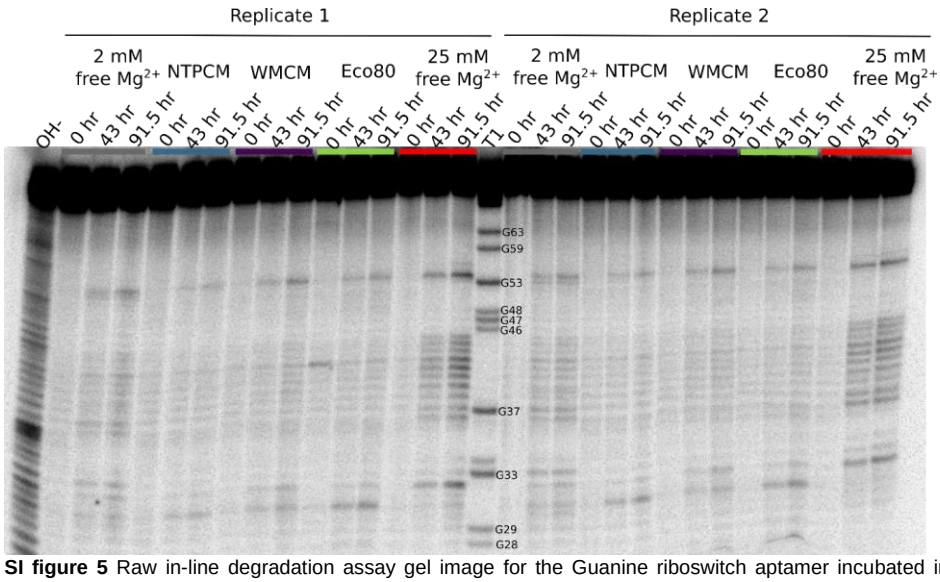

SI figure 5 Raw in-line degradation assay gel image for the Guanine riboswitch aptamer incubated in artificial cytoplasms at 37 °C and pH 7. The OH- lane contains a hydrolysis ladder which cleaves after every nucleotide and T1 contains the RNA treated with T1 ribonuclease which cleaves after every G. Enough Mg^{2+} was added to each artificial cytoplasm to have 2 mM Mg^{2+} free as determined in Figure 1. Nucleotides 28 to 63 were quantified. Cleavage fragments shorter than 28 could not be quantified because of band smearing due to the high concentration of charged molecules in the samples and cleavage fragments longer than 63 could not be resolved.

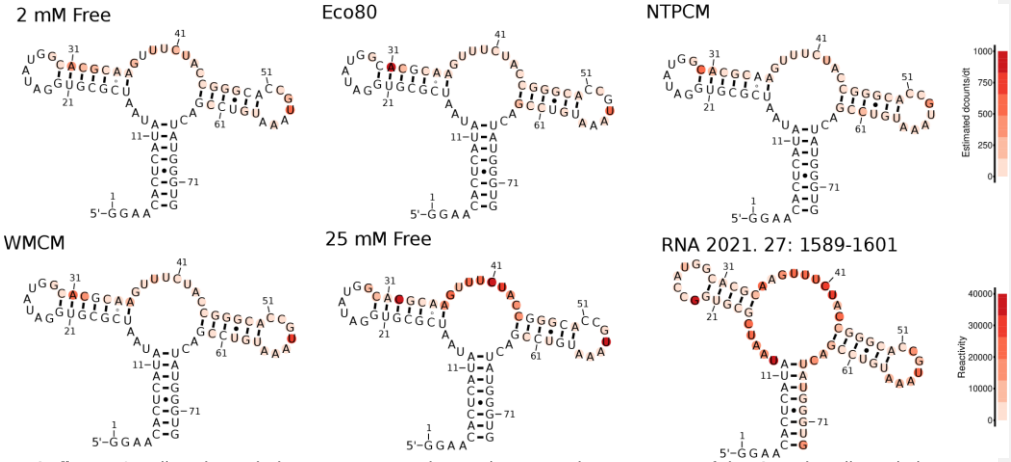

SI figure 6 In-line degradation rates mapped onto the secondary structure of the Guanine riboswitch aptamer.

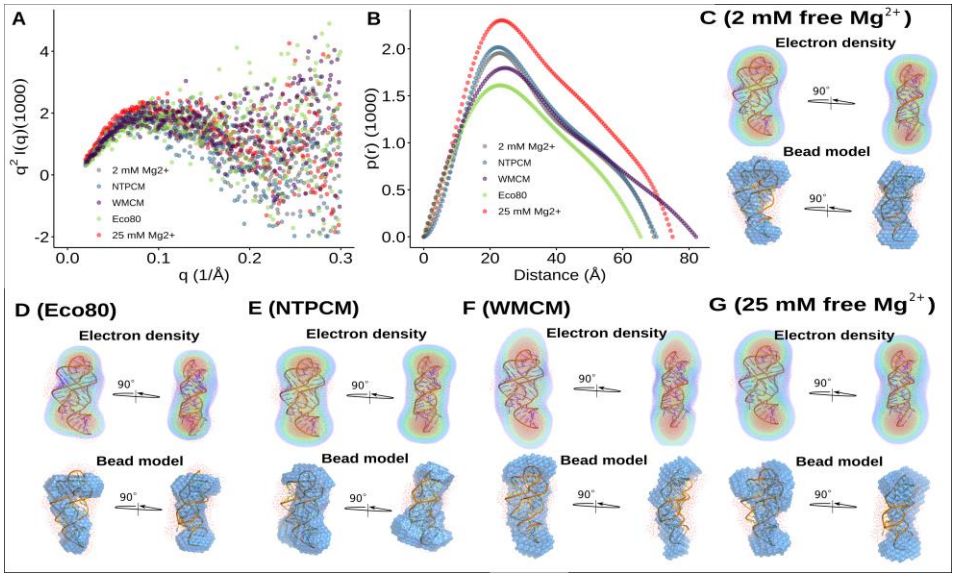

SI figure 7 Small angle x-ray scattering (SAXS) indicates that the guanine riboswitch aptamer adopts a similar structure in 2 mM free Mg^{2+}, Eco80, NTPCM, WMCM and 2 mM free Mg^{2+}.

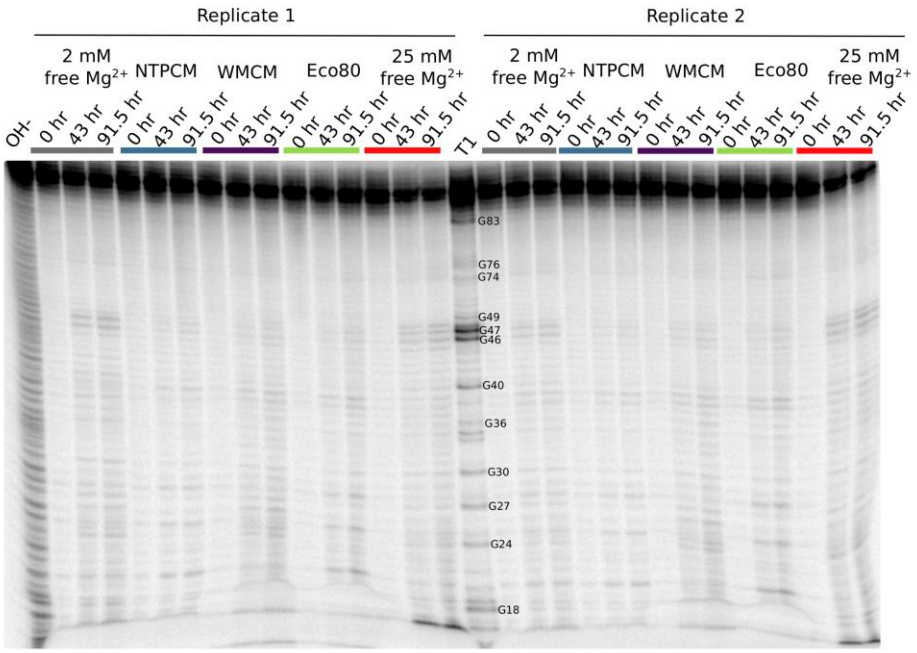

SI figure 8 Raw in-line degradation assay gel image for the cleaved CPEB3 ribozyme incubated in artificial cytoplasms at 37 °C and pH 7. The OH- lane contains a hydrolysis ladder which cleaves after every nucleotide and T1 contains the RNA treated with T1 ribonuclease which cleaves after every G. Enough Mg^{2+} was added to each artificial cytoplasm to have 2 mM Mg^{2+} free as determined in Figure 1. Nucleotides 28 to 63 were quantified. Cleavage fragments shorter than 28 could not be quantified because of band smearing due to the high concentration of charged molecules in the samples and cleavage fragments longer than 63 could not be resolved.

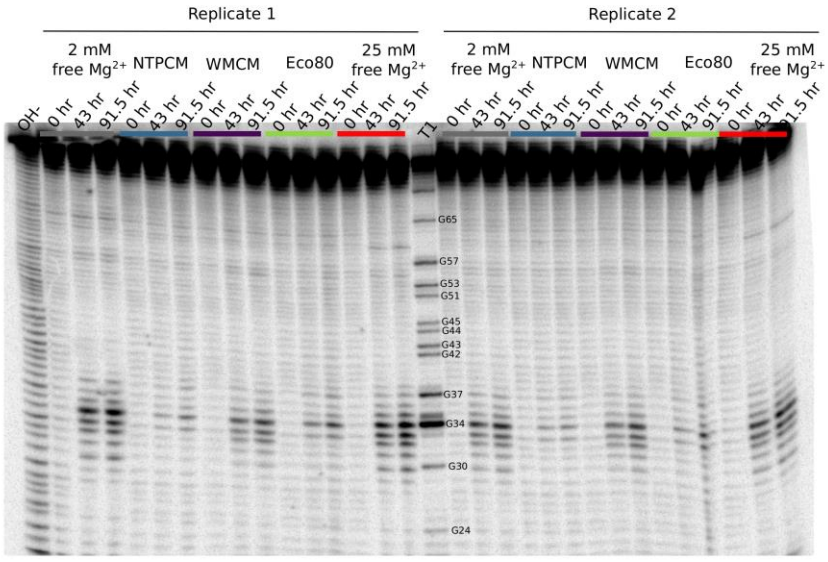

SI figure 9 Raw in-line degradation assay gel image for the cleaved tRNAphe ribozyme incubated in artificial cytoplasms at 37 °C and pH 7. The OH- lane contains a hydrolysis ladder which cleaves after every nucleotide and T1 contains the RNA treated with T1 ribonuclease which cleaves after every G. Enough Mg2+ was added to each artificial cytoplasm to have 2 mM Mg2+ free as determined in Figure 1. Nucleotides 28 to 63 were quantified. Cleavage fragments shorter than 28 could not be quantified because of band smearing due to the high concentration of charged molecules in the samples and cleavage fragments longer than 63 could not be resolved.

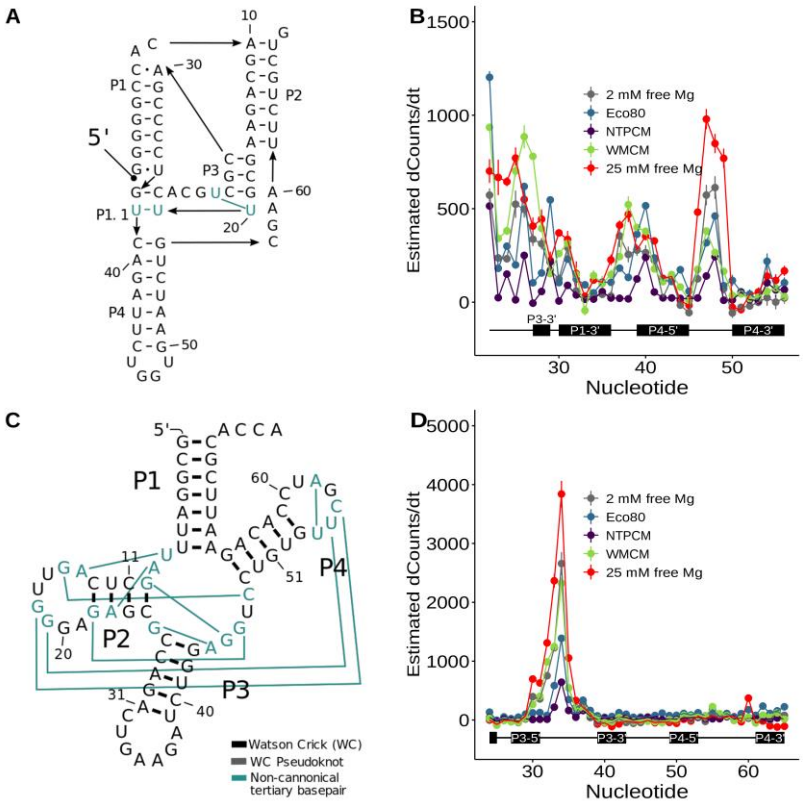

SI figure 10 E. coli metabolite and Mg^{2+} mixtures stabilize the chemical structure of RNA. (A) Secondary structure of the cleaved CPEB3 ribozyme with tertiary contacts represented by colored lines. (B) Degradation rate, by the increase in counts with time at each residue, in different solution conditions as a function of location in the cleaved CPEB3 ribozyme. Points represent the slope for the line of best fit of counts versus time and error bars represent the standard error in the slope estimated from the fit. (C) Secondary structure of yeast tRNAphe with tertiary contacts represented by colored lines. (D) Degradation rate, by the increase in counts with time at each residue, in different solution conditions as a function of location in the tRNAphe . Points represent the slope for the line of best fit of counts versus time and error bars represent the standard error in the slope estimated from the fit.

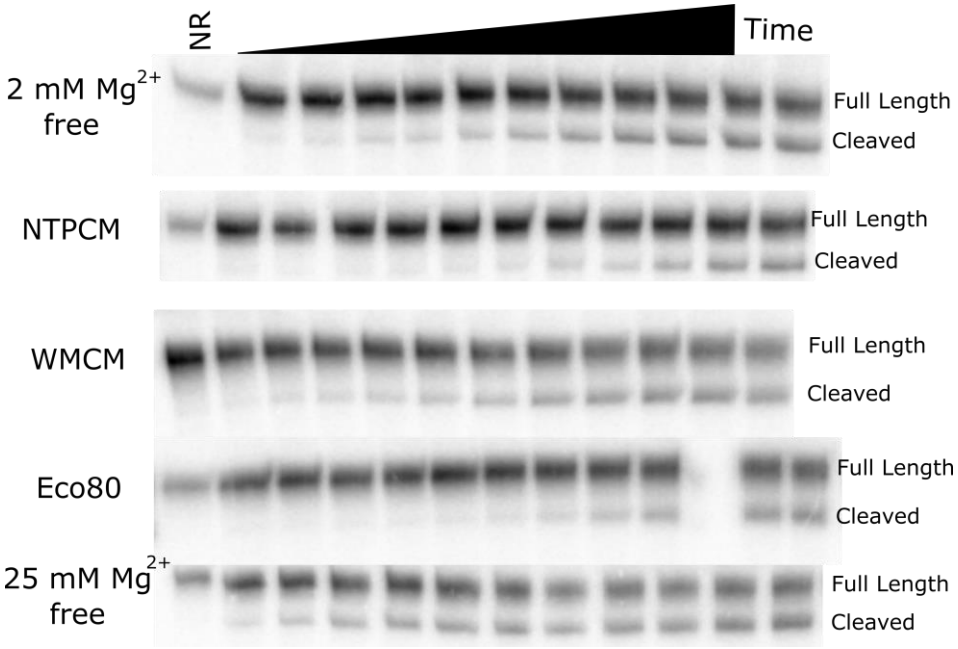

SI figure 11 CPEB3 ribozyme kinetics denaturing polyacrylamide gel images.

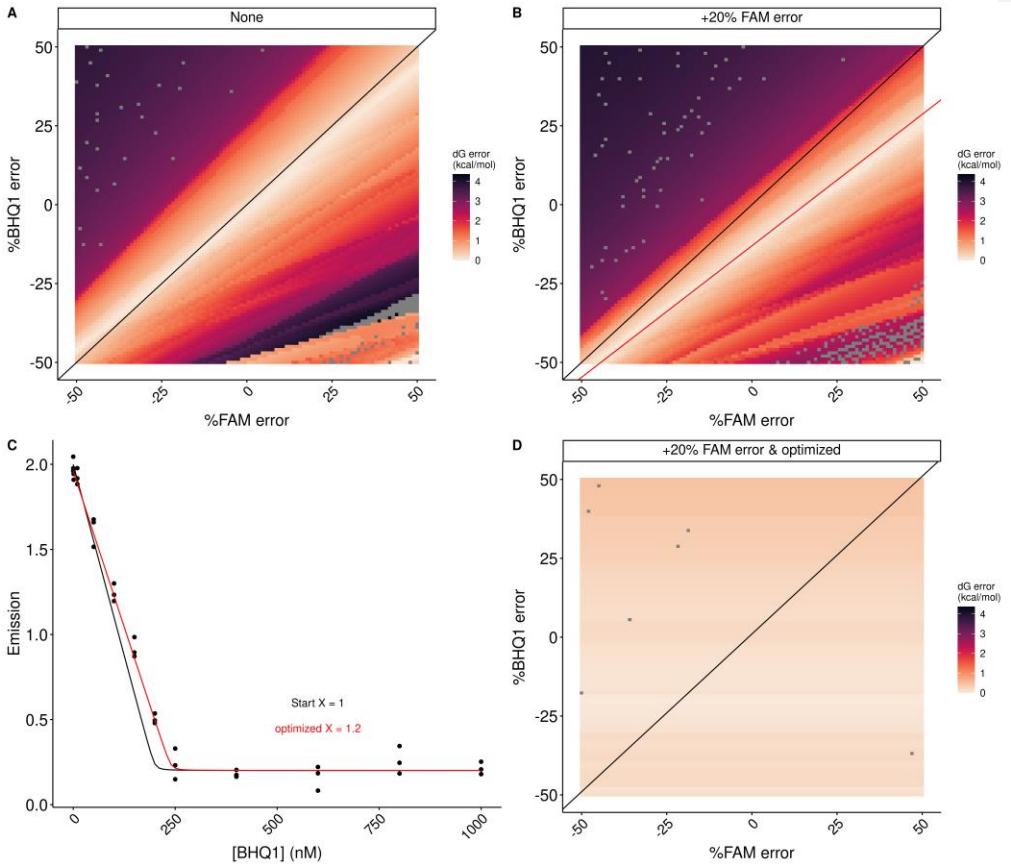

SI figure 12 The concentration optimization algorithm improves the accuracy of helix folding energies calculated with MeltR using data with inaccurate RNA concentration estimates. (A) Error in the Gibbs free energy (dG) calculated with MeltR on modeled data assuming perfectly accurate RNA concentration estimates is reduced when the %FAM-RNA concentration error and %RNA-BHQ1 concentration error compensates according to the black line, %FAM-RNA error = %RNA-BHQ1. Data were modeled assuming a folding enthalpy (ΔH), entropy (ΔS), and Gibb's free energy at 37 °C (ΔG) of -56.2 kcal/mol, -136. 4 cal/mol/K, and -13.9 kcal/mol respectively, and 5% random fluorescence error. Concentration errors were seeded into the modeled data and the data was fit with MeltR. (B) Error in the Gibbs free energy (dG) calculated with MeltR on modeled data, assuming a +20% FAM-RNA concentration estimate, is reduced when the %FAM-RNA concentration error and %RNA-BHQ1 concentration error compensate according to the red line, %RNA-BHQ1 = X*%FAM-RNA error + (100 – 100*X)/X, where X is the factor the MeltR concentration optimization algorithm multiplies the FAM-RNA concentration estimate by. Data were modeled assuming a folding ΔH, ΔS, and ΔG of -56.2 kcal/mol, -136. 4 cal/mol/K, and -13.9 kcal/mol respectively, 5% random fluorescence error, and a +20% increase in the FAM-RNA concentration. Additional concentration errors were seeded into the modeled data and the data was fit with MeltR. (C) MeltR identifies the FAM-RNA concentration correction factor (X) using a low temperature fluorescence isotherm as a Job plot. Black data points represent modeled fluorescence data from B at 20 °C. The black line represents the shape of the curve with a X of 1. The red line represents the shape of the curve with an optimized X of 1.2. (D) Error in the Gibbs free energy (dG) calculated with MeltR using the concentration optimization algorithm and the data from B. On average, MeltR estimates the correct ΔG within 0.2 kcal/mol, using the concentration optimization algorithm.

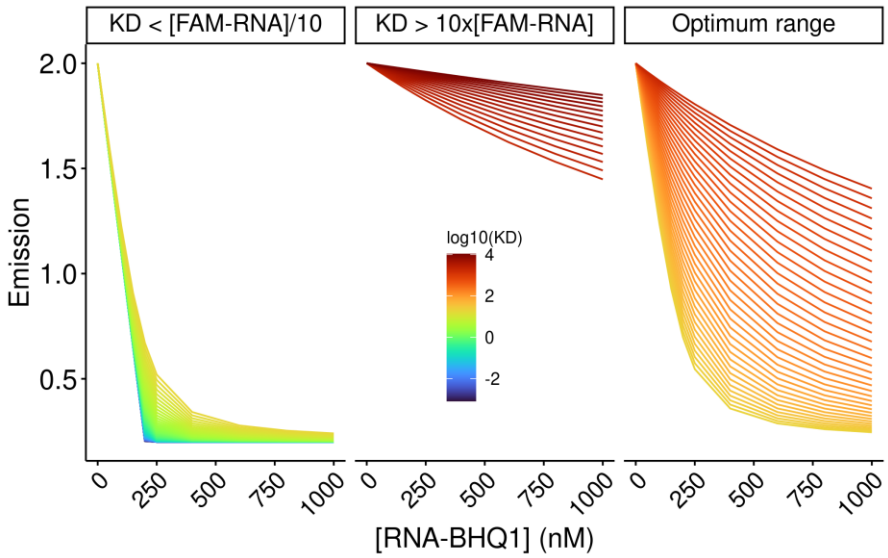

SI figure 13 K_Ds calculated using MeltR are most accurate between the FAM-RNA concentration/10 and 10 times the FAM-RNA concentration. At K_Ds that are more than 10 fold lower than the FAM-RNA concentration, the shape of the curve is independent of the K_D. At K_Ds more than 10 fold higher than the FAM-RNA concentration, there is very little dependence of FAM-RNA emission on RNA-BHQ1 concentration. However, the curve shape is highly dependent on K_D within the optimum range, so MeltR allows the user to specify an optimum K_D range to calculate helix folding energies.

Supplementary information tables

SI table 1 Recipe for a 2x stock solution of the Eco80 artificial cytoplasm. Prepare in a 10 mL volumetric flask.

Step 1 mass reagents into a 10 mL volumetric flask							
Reagent	Vendor (product #)	Purity	Molar mass (g/mL)	2x[Ligand] (mM)	Mass or volume	Na^+ added (mM)	K^+ added (mM)
Adenine triphoshate disodium salt hydrate	Sigma-Aldrich A2383	≥99%	551.14	19.26	525 µL of 367 mM	38.52	
Uridine triphoshate trisodium salt	Alpha-Azar J63427	≥98%	550.09	16.58	448 µL of 370 mM	49.74	
Guanosine triphoshate trisodium salt	Sigma-Aldrich G8877	≥95%	523.18	9.74	380 µL of 256 mM	29.22	
Deoxythymidine triphoshate disodium salt	Thermo R0171	≥99%	solution	9.24	924 µL of 100 mM	18.48	
L-glutamic acid potassium salt monohydrate	Millipore Sigma G1501	≥99%	203.23	192	0.3902 g		192
Glutathione, reduced, free acid	Cal biochem 3541	≥98%	307.32	33.2	0.102 g		
D-Fructose-1,6-bisphosphate trisodium salt hydrate	Sigma-Aldrich F6803	≥98%	406.06	30.4	217 µL of 1400 mM	91.2	
Uridine 5'-diphospho-N-acetylglucosamine disodium salt	Sigma-Aldrich U4375	≥98%	651.32	18.48	313 µL of 591 mM	36.96	
D-Glucose 6-phosphate dipotassium salt hydrate	Sigma-Aldrich G7375	≥98%	336.32	15.76	157 µL of 1001 mM		31.52
L-aspartic acid dipotassium salt	Millipore Sigma A9256	≥98%	133.10	8.46	66 µL of 1276 mM		16.92
L-valine monopotassium salt	Sigma Aldrich V0500	≥98%	117.15	8.04	80 µL of 1000 mM		16.08
L-glutamine monopotassium salt	Sigma G3126	≥99%	146.14	7.62	43 µL of 1759 mM		7.62
6-Phosphogluconic acid trisodium salt	Sigma-Aldrich P6888	≥95%	342.08	7.54	90 µL of 839 mM	22.62	
Sodium pyruvate	Sigma P8574	≥99%	110.04	7.32	121 µL of 606 mM	7.32	
dihydroxyacetone phosphate hemi magnesium salt	Sigma 51296	≥95%	180.19	6.12	54 µL of 1128 mM		
MOPS	Sigma-Aldrich M3183	≥99.5	209.26	20	41.9 g		
EDTA	IBI scientific IB70182	≥99%	372.24	0.01	1 µL of 100 mM tetrasodium solution	0.04	
SDS	JT Baker 4095-04	≥99%	288.38	0.035 (0.001%)	10 µL of 35 mM (1%)	0.035	
Step 2 Add acid or base to to pH 7.0							
Reagent	Vendor (product #)	Purity	Molar mass (g/mL)	2x[Ligand] (mM)	Mass or volume	Na^+ added (mM)	K^+ added (mM)
Sodium hydroxide	Millipore Sigma Sx0593	≥97%	40.00	NA	100 µL of 10 M	100	
Potassium hydroxide	JT Baker 3140-11	≥85%	56.11	NA	0 µL of 5 M		
Step 3 Calculate how much Na^+ and K^+ was added							
					Sum	Na^+ (mM)	K^+ (mM)
					Total monovalent added (mM)	394.135	264.14
Step 4 Add NaCl and KCl for a total final monovalent concentration of 480 mM Na^+ and 280 mM K^+							
Reagent	Vendor (product #)	Purity	Molar mass (g/mL)	2x[Ligand] (mM)	Mass or volume	Na^+ added (mM)	K^+ added (mM)
Sodium chloride	Dot Scientific DSS23020	≥99%	58.4		171.7 µL of 5 M	85.865	

Potassium chloride	Millipore Sigma P9541	≥99%	74.55		79.3 µL of 2 M		15.86
Step 5 Fill to 10 mL in a volumetric flask and 2 µm filter							
Step 6 Check 1xConcentrated pH							
						Final pH	6.99

SI Table 2 Apparent binding constants determined with Isothermal titration calorimetry (ITC).

Metabolite	Syringe (mM)	Cell (mM)	ΔH (kcal/mol)	K' (M^{-1})	K_D' (mM^{-1})
ATP	15 mM $MgCl_2$[a]	0.1 mM ATP[a]	1.83 (0.04)	3600 (200)	0.28 (0.01)
UTP	15 mM $MgCl_2$[a]	0.2 mM UTP[a]	1.70 (0.01)	4200 (70)	0.248 (0.004)
GTP	15 mM $MgCl_2$[a]	0.2 mM GTP[a]	1.43 (0.02)	5000 (200)	0.201 (0.007)
dTTP	15 mM $MgCl_2$[a]	0.2 mM dTTP[a]	2.19 (0.02)	6300 (300)	0.160 (0.003)
Fructose 1,6-BP	100 mM $MgCl_2$[a]	5.0 mM Fructose 1,6-BP[a]	0.414 (0.004)	169 (4)	5.9 (0.1)
UDP-GlcNAC	100 mM $MgCl_2$[a]	5.0 mM UDP-GlcNAC	0.57 (0.02)	34 (2)	29 (2)
Glucose 6-P	100 mM $MgCl_2$[a]	5.0 mM Glucose 6-P[a]	0.555 (0.003)	57.9 (0.7)	17.3 (0.2)
6-P-gluconic acid	100 mM $MgCl_2$[a]	5.0 mM 6-P-gluconic acid[a]	0.662 (0.005)	70 (1)	14.4 (0.2)
Dihydroxyacetone phosphate	100 mM $MgCl_2$[a]	5.0 mM dihydroxy-acetone phosphate[a]	0.50 (0.01)	51 (3)	20 (1)
EDTA	6 mM $MgCl_2$[a]	1.5 mM EDTA 1.0 mM $MgCl_2$[a,b]	2.85 (0.04)	220,000 (30,000)	0.0045 (0.0006)

[a]240 mM NaCl 140 mM KCl 10 mM HEPES pH 7.0 at 37 °C
[b]Mg^{2+} and EDTA were incorporated into the cell in order to sequester trace tight binding metal ions and thereby negate their contribution to ITC signal.

SI Table 3 Apparent metabolite-Mg^{2+} binding constants determined with HQS emission. F_{max}, F_{min}, and K_{HQS} are determined by fitting HQS emission in the absence of chelators and used to calculate the free Mg^{2+} concentration in each sample. Metabolite binding constants, K' and K_D'. are determined by fitting the relationship between the free Mg^{2+} concentration and the total $MgCl_2$ concentration using SI Equation 4.

Metabolite	F_{max}	F_{min}	K_{HQS} (mM^{-1})	K' (mM^{-1})	K_D' (mM^{-1})
L-Glutamic acid	187,000 (1000)	0 (810)	0.281 (0.008)	0.0019 (0.0002)	520 (50)
Glutathione	182,000 (1000)	592 (750)	0.279 (0.007)	NA[c]	NA[c]
L-Aspartic acid	196,000 (1000)	0 (820)	0.283 (0.007)	0.0021 (0.0001)	465 (12)
L-Valine	188,200 (800)	495 (580)	0.274 (0.005)	NA[c]	NA[c]
L-Glutamine	190,000 (1400)	516 (110)	0.27 (0.01)	NA[c]	NA[c]
Pyruvic acid	188,000 (1500)	0 (1300)	0.35 (0.01)	0.063 (0.003)	15.8 (0.9)

[c]No binding observed as per SI Figure 2

SI Table 4 HQS fits in the absence of chelators, used to determine free Mg^{2+} concentrations. F_{max}, F_{min}, and K_{HQS} are determined by fitting HQS emission in the absence of chelators and used to calculate the free Mg^{2+} concentration in each sample.

Metabolite	F_{max}	F_{min}	K_{HQS} (mM^{-1})
Eco80	185,100 (800)	124 (1000)	0.239 (0.005)
NTPCM	187,000 (1500)	436 (1000)	0.26 (0.01)
WMCM	179,000 (1600)	0 (1400)	0.32 (0.01)

SI table 5 Stability of RNA helices in *E. coli* metabolite mixtures. Helix energy was calculated by fitting raw fluorescence data with MeltR. Standard errors are estimated from fits. Extra significant digits are included to avoid propagating rounding errors.

Sequence[a]	Condition[b]	X[e]	Method 1 VH plot ΔH kcal/mol	Method 1 VH plot ΔS cal/mol/K	Method 1 VH plot ΔG kcal/mol	Method 2 Global fit ΔH kcal/mol	Method 2 Global fit ΔS cal/mol/K	Method 2 Global fit ΔG kcal/mol	%Diff.[d] ΔG	%Diff.[d] ΔS	%Diff.[d] ΔG
1:CGCAUCCU/ AGGAUGCG	2 mM free	1.3	-55.9 (0.2)	-136.0 (0.7)	-13.82 (0.01)	-56.0 (8.9)	-135.9 (27.0)	-13.8 (0.5)	0.2%	0.1%	0.1
	NTPCM	2	-52.2 (0.4)	-125 (1)	-13.41 (0.02)	-52.4 (7.6)	-125.6 (23.2)	-13.4 (0.4)	0.4%	0.5%	0.1%
	WMCM	1.0	-61.4 (0.8)	-152 (2)	-14.22 (0.05)	-61.1 (14.0)	-151.2 (42.5)	-14.2 (0.9)	0.5%	0.5%	0.1%
	Ecoli80	1.5	-44.5 (0.7)	-102 (2)	-12.70 (0.04)	-44.4 (7.6)	-102.1 (23.3)	-12.7 (0.4)	0.2%	0.1%	0.0%
2: CCAUAUCA/ UGAUAUGG	2 mM free	0.9	-53.4 (1.0)	-133 (3)	-12.02 (0.04)	-52.3 (14.9)	-129.9 (43.2)	-12.0 (0.5)	2.1%	2.4%	0.2%
	NTPCM	1.3	-42.9 (0.5)	-101 (1)	-11.50 (0.02)	-42.4 (20.4)	-99.6 (63)	-11.5 (0.8)	1.2%	1.4%	0.0%
	WMCM	1.0	-53 (2)	-132 (7)	-11.9 (0.1)	-51.6 (5.3)	-128.0 (1.6)	-11.9 (0.2)	2.7%	3.1%	0.0%
	Ecoli80	0.9	-57 (2)	-146 (5)	-11.38 (0.05)	-54.0 (13.1)	-137.7 (-41.1)	-11.3 (0.4)	5.4%	5.9%	0.7%
3:CCAUAUUA/ UAAUAUGG	2 mM free	0.9	-53.5 (0.4)	-137 (1)	-10.76 (0.01)	-53.2 (8.4)	-136.7 (27.1)	-10.8 (0.1)	0.6%	0.2%	0.4%
	NTPCM	1.0	-45.0 (0.2)	-112.5 (0.5)	-10.158 (0.002)	-45.0 (8.0)	-112.2 (25.6)	-10.2 (0.1)	0.0%	0.3%	0.4%
	WMCM	0.8	-43 (2)	-107 (5)	-9.94 (0.02)	-40.5 (9.3)	-98.4 (29.6)	-9.9 (0.1)	6.0%	8.4%	0.4%
	Ecoli80	1.2	-41.3 (0.2)	-100.4 (0.7)	-10.15 (0.01)	-41.2 (9.2)	-100.3 (29.4)	-10.2 (0.2)	0.2%	0.1%	0.5%
4:CGGAUGGC/GCCA UCCG	2 mM free	1.1	-71.1 (0.8)	-179 (2)	-15.6 (0.06)	-71.3 (15.6)	-179.6 (46.6)	-15.6 (1.1)	0.3%	0.3%	0%
	NTPCM	1.2	-70.4 (0.6)	-177 (2)	-15.28 (0.05)	-70.5 (15.1)	-178.0 (45.2)	-15.3 (1.0)	0.1%	0.6%	0.1%
	WMCM	1.1	-65.5 (2)	-162 (7)	-15.2 (0.2)	-65.3 (12.2)	-161.6 (36.4)	-15.2 (0.9)	0.3%	0.2%	0%
	Ecoli80	1.0	-69.7 (0.8)	-176 (3)	-15.0 (0.1)	-69.6 (11.4)	-176.3 (34.2)	-15.0 (0.8)	0.1%	0.2%	0.2%
5:CGUAUGUA/ UACAUACG	2 mM free	0.8	-63.2 (0.9)	-169 (3)	-10.85 (0.02)	-62.3 (7.3)	-165.9 (23.0)	-10.8 (0.1)	1.4%	1.9%	0.5%
	NTPCM	0.9	-59 (1)	-157 (4)	-10.30 (0.01)	-58.5 (7.6)	-155.5 (24.3)	-10.3 (0.1)	0.9%	1.0%	0.0%
	WMCM	1.0	-67 (1)	-180 (3)	-10.85 (0.02)	-66.1 (10.5)	-178.1 (33.2)	-10.8 (0.2)	1.4%	1.1%	0.1%
	Ecoli80	1.0	-61 (1)	-164 (3)	-10.41 (0.01)	-60.9 (4.09)	-162.9 (13.1)	-10.4 (0.06)	0.2%	0.7%	0.2%
Average %error			1.7%	2.0%	0.3%	21.7%	26.5%	3.4%	1.2%	1.4%	0.2%

[a]The first sequence was 5'-FAM labeled and the second sequence was 3'-BHQ1 labeled.
[b]All solutions contain 2 mM Free Mg, 240 Na^+ 140 mM K^+.
[c]Concentration optimization factor used to correct FAM-RNA concentrations by MeltR.
[d]Percent difference between Method 1 and Method 2.

SI Table 6 Radius of gyration analysis

Supplementary References